Magnetic anisotropy in the Fe(II)Fe(III) bimetallic oxalates

Randy S. Fishman and Fernando A. Reboredo
Materials Science and Technology Division, Oak Ridge National Laboratory, Oak Ridge, Tennessee 37831-6065, USA
(Received 7 January 2008; published 23 April 2008)

Bimetallic oxalates are layered molecule-based magnets with transition metals M(II) and M'(III) coupled by oxalate molecules ox=C_2O_4 in an open honeycomb structure. Among the most interesting molecule-based magnets, Fe(II)Fe(III) bimetallic compounds with spins $S=2$ and $S'=5/2$ ferrimagnetically order at a transition temperature T_c that ranges from 30 to 48 K, depending on the organic cation between the layers. In small magnetic fields, several of these compounds exhibit "giant negative magnetization" below a compensation temperature of about $0.62T_c$. By studying the behavior of the low-energy orbital doublet produced by a C_3-symmetric crystal field, we construct a reduced Hamiltonian that contains both the exchange and spin-orbit interactions. This Hamiltonian is used to explain almost all of the important behaviors of the Fe(II)Fe(III) bimetallic oxalates, including the stability of magnetic order in weakly coupled layers and the magnetic compensation in compounds with high transition temperatures. In a magnetic field perpendicular to the bimetallic layers, a spin-flop transition is predicted at a field of about $3J_c/\mu_B \approx 24$ T, where $J_c \approx 0.45$ meV is the nearest-neighbor antiferromagnetic exchange coupling. Holstein–Primakoff $1/S$ and $1/S'$ expansions are used to evaluate the spin-wave spectrum and to estimate the spin-wave gap $\Delta_{sw} \approx 1.65$ meV in compounds that exhibit magnetic compensation. We predict that the negative magnetization can be optically reversed by near-infrared light. Breaking the C_3 symmetry about each of the Fe(II) ions through either a cation-induced distortion or uniaxial strain in the plane of the bimetallic layer is predicted to increase the magnetic compensation temperature.

DOI: 10.1103/PhysRevB.77.144421 PACS number(s): 75.50.Xx, 71.70.Ej, 75.10.Dg, 75.30.Gw

I. INTRODUCTION

Astounding progress has been achieved[1,2] during the past two decades in the synthesis and characterization of molecule-based magnets. Comparatively little progress has been made in predicting their magnetic behavior. This paper closes that gap by constructing a theoretical framework that can be used to design the magnetic properties of an important class of layered molecule-based magnets. Based on the symmetry of the crystal-field potential and the energy scales of the spin-orbit and exchange interactions, we evaluate the magnetization, the magnetic phase diagram, and the spin-wave (SW) spectrum of the Fe(II)Fe(III) bimetallic oxalates. Due to the sensitivity of the crystal-field potential to changes in the organic constituents, the magnetic properties of this layered molecule-based magnet can be finely controlled.

First synthesized in 1992,[3] bimetallic oxalates are salts with the chemical formula $A[M(\mathrm{II})M'(\mathrm{III})(\mathrm{ox})_3]$. Each of the metallic layers contains two different metal atoms in the alternating honeycomb structure pictured in Fig. 1, with nearest-neighbor separations a of about 5.4 Å.[4–6] The neighboring metal atoms M(II) with valence of +2 and M'(III) with valence of +3 are connected by the oxalate molecule ox=C_2O_4 with valence of −2. Most commonly, M(II)=Mn, Ni, Fe, Co, Cu, or Zn and M'(III)=V, Cr, Mn, or Fe. The negatively charged bimetallic layers are separated by an organic cation A with a charge of +1. Depending on the metal and organic cation species, the stacking of the bimetallic planes can be rather complex with two to six bimetallic layers per unit cell.[4,5]

For different metal atoms, a single bimetallic layer can be either ferromagnetic [M(II) and M'(III) moments aligned] or ferrimagnetic [M(II) and M'(III) moments opposite]. In zero field, the magnetic moments of M(II) and M'(III) point out of the plane. While it does not change the sign of the exchange coupling, the choice of organic cation A affects the overall behavior of the system. Depending on the organic cation, bimetallic oxalates can be optically activated,[5] metallic,[7] or disordered.[6,8]

Some of the highest magnetic transition temperatures T_c among the bimetallic oxalates are found in the ferrimagnetic Fe(II)Fe(III) compounds,[9–13] where Fe(II) and Fe(III) have $3d^6$ and $3d^5$ electronic configurations, respectively. By Hund's first rule, the spins on the Fe(II) and Fe(III) sites are $S=2$ and $S'=5/2$. Since the Fe(III) shell is half-filled, only the Fe(II) moments experience a magnetically anisotropic

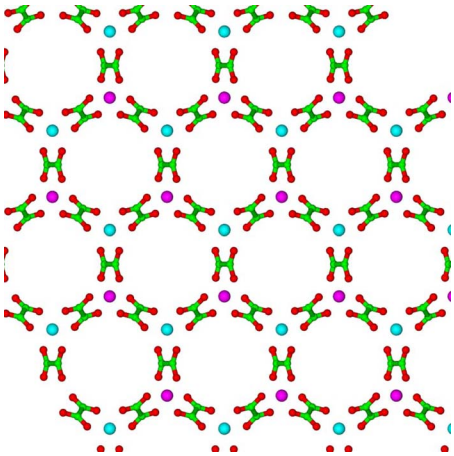

FIG. 1. (Color online) A bimetallic layer with M(II) (purple) and M'(III) (blue) in an open honeycomb structure coupled by oxalate C_2O_4 molecules, with oxygen atoms in red and carbon atoms in green.

environment due to the spin-orbit coupling and crystalline field.

In small magnetic fields of roughly 100 Oe, Fe(II)Fe(III) compounds with certain organic cations exhibit "giant negative magnetization" (GNM): the magnetization points along the field direction just below the ferrimagnetic transition of about 45 K but it changes sign below the compensation temperature of about 28 K. At low temperatures, the nearly saturated magnetization points opposite to the magnetic field. Magnetic compensation in ferrimagnets occurs when the contributions of the different magnetic sublattices cancel each other. This behavior is commonly attributed to the next-nearest-neighbor interactions between spins on the same sublattice.[14] However, the large separation between the metal atoms on the open honeycomb structure suggests that the next-nearest-neighbor interactions should be rather weak in the bimetallic oxalates.

Whereas some Fe(II)Fe(III) compounds exhibit GNM, others do not. Compounds with cations $A=\mathrm{N}(n\text{-}\mathrm{C}_3\mathrm{H}_7)_4$, $\mathrm{P}(\mathrm{C}_6\mathrm{H}_5)_4$, or $\mathrm{As}(\mathrm{C}_6\mathrm{H}_5)_4$ exhibit "normal" magnetic behavior without magnetic compensation while compounds with $A=\mathrm{N}(n\text{-}\mathrm{C}_n\mathrm{H}_{2n+1})_4$ $(n=4$ or $5)$, $\mathrm{N}(\mathrm{C}_6\mathrm{H}_5\mathrm{CH}_2)(n\text{-}\mathrm{C}_4\mathrm{H}_9)_3$, $(\mathrm{C}_6\mathrm{H}_5)_3\mathrm{PNP}(\mathrm{C}_6\mathrm{H}_5)_3$, $\mathrm{P}(n\text{-}\mathrm{C}_4\mathrm{H}_9)_4$, CoCp_2^*, or FeCp_2^* exhibit GNM with a single compensation temperature.[9–12] Recently, Tang *et al.*[13] studied an Fe(II)Fe(III) bimetallic oxalate with $A=\mathrm{N}(n\text{-}\mathrm{C}_4\mathrm{H}_9)_4$ that passes through two compensation temperatures. GNM compounds have higher transition temperatures and Curie constants than normal compounds. Part of our motivation was to understand why some Fe(II)Fe(III) compounds exhibit magnetic compensation but others do not.

The effects of the bimetallic layer separation l can be systematically controlled in the Fe(II)Fe(III) bimetallic oxalates with $A=\mathrm{N}(n\text{-}\mathrm{C}_n\mathrm{H}_{2n+1})_4$: as n increases from 3 to 5, l grows from 8.2 to 10.2 Å.[10] If the interlayer coupling was required for magnetic order, then the transition temperature would decrease as l increases. Instead, T_c actually increases from 35 to 48 K with growing layer separation (T_c may be suppressed by the breaking of C_3 symmetry when l is small). Other evidence of the role of interlayer coupling comes from the observation[7,15] that the magnetic $s=1/2$ cation FeCp_2^* hardly changes the transition temperature and coercive field of a wide range of bimetallic oxalates.

These experiments suggest that the interlayer coupling is not primarily responsible for the magnetic ordering of well-separated bimetallic planes. However, according to the Mermin–Wagner theorem, gapless spin excitations in an isolated two-dimensional layer will destroy long-range magnetic order at nonzero temperatures. Two-dimensional magnetic order will survive at nonzero temperatures only if the SW excitation spectrum is gapped by the effects of magnetic anisotropy.[16] We demonstrate that the anisotropy associated with the spin-orbit coupling and crystalline field within each layer can explain the stability of magnetic order at nonzero temperatures of an isolated bimetallic plane.

This paper is divided into seven sections. Section II employs symmetry and energy considerations to derive the C_3-symmetric crystal-field splitting of the Fe(II) orbitals. The lowest-energy eigenstates of the crystal-field Hamiltonian are used to evaluate the transition temperature and magnetization in Sec. III. Section IV is devoted to a treatment of the magnetic susceptibility at high temperatures and the magnetic phase diagram at low temperatures. Using a Holstein–Primakoff expansion about the classical-spin limit, the SW frequencies are derived in Sec. V. Section VI discusses the effects of a non-C_3-symmetric distortion of the local crystal field around each Fe(II) ion. Finally, Sec. VII contains a summary and a discussion of future prospects. Some results were previously presented in Ref. 17.

II. CRYSTAL-FIELD SPLITTING

We assume that Fe(II)Fe(III) bimetallic oxalates are characterized by a hierarchy of three energy scales.[14,18] Since it originates in the Pauli exclusion principle on each transition metal, the Hund coupling that fixes the spins $S=2$ and $S'=5/2$ on the Fe(II) $(3d^6)$ and Fe(III) $(3d^5)$ sites is the dominant energy. Indeed, susceptibility measurements[10] confirm that both Fe(II) and Fe(III) are in their high-spin states. The C_3-symmetric contribution V of the crystal-field potential produced by the six oxygen atoms around each Fe atom is next in importance. Finally, the antiferromagnetic exchange coupling $J_c\mathbf{S}\cdot\mathbf{S}'$ between the Fe(II) and Fe(III) spins, the spin-orbit coupling $\lambda\mathbf{L}\cdot\mathbf{S}$ on the Fe(II) sites [$\lambda<0$ because the Fe(II) shell is more than half-filled], and any non-C_3-symmetric distortions of the crystal field are assumed to be much smaller than the C_3-symmetric crystal-field potential V but may be of comparable magnitude with each other. Whereas the Fe(II) shell is equivalent to a single electron in an $L=2$ orbital, there is no spin-orbit coupling on the Fe(III) sites because the Fe(III) shell is half-filled.

As shown by x-ray measurements[4,5] and pictured in Ref. 17, the positions of the oxygen atoms around each transition metal are well approximated by two equilateral triangles, one above and the other below the bimetallic plane. One triangle lies a little closer to the transition metal and is a little larger than the other triangle, which is rotated by about 48° from the first. Within each bimetallic plane, the helicities around the Fe(II) and Fe(III) sites are opposite. The C_3-symmetric crystal field $V(\rho,\theta,\phi)$ at each Fe(II) site can be expanded in Legendre polynomials as

$$V(\rho,\theta,\phi)=\sum_{n\geq 0,n'\geq 0,n+3n'>1} A_{n,n'}\rho^{n+3n'}P_n(\cos\theta)\times\cos(3n'\phi+\mu_{n,n'}), \quad (1)$$

where the linear $(n=1,\ n'=0)$ term in the radial component ρ must vanish since no net force may act on the Fe(II) ion, which is in its equilibrium position. The phases $\mu_{n,n'}$ reflect the rotation of the two oxygen triangles above and below each Fe(II) site.

Upon integrating over the spherical coordinates, we find that the crystal-field Hamiltonian $\underline{H}^{\mathrm{cf}}=\langle m'|V(\rho,\theta,\phi)|m\rangle$ $(m',m=\pm 2,\pm 1,0)$ of the $L=2$ Fe(II) orbitals can be written as

$$\underline{H}^{\rm cf} = \begin{pmatrix} \gamma & 0 & 0 & \alpha & 0 \\ 0 & \gamma' & 0 & 0 & -\alpha \\ 0 & 0 & 0 & 0 & 0 \\ \alpha^* & 0 & 0 & \gamma' & 0 \\ 0 & -\alpha^* & 0 & 0 & \gamma \end{pmatrix}, \tag{2}$$

which subtracts off the diagonal matrix $\langle 0|V|0\rangle \underline{I}$. The $n=2,4$ and $n'=0$ terms in $V(\rho,\theta,\phi)$ produce the diagonal γ and γ' terms, which are real; the $n'=1$ terms produce the off-diagonal α terms, which couple the $L=2$ wave functions with $m-m'=\pm 3$ and may be complex due to the phases $\mu_{n,1}$ in Eq. (1).

After diagonalizing $\underline{H}^{\rm cf}$, we obtain the eigenstates $|\psi_1\rangle \propto -2\alpha|2\rangle+(\gamma-\gamma'+r)|-1\rangle$ and $|\psi_2\rangle \propto 2\alpha|1\rangle+(-\gamma+\gamma'+r)|-2\rangle$, which constitute an orbital doublet with degenerate energies $\epsilon_1=\epsilon_2=\epsilon^{(0)}\equiv(\gamma+\gamma')/2-r/2$, where $r=\sqrt{(\gamma-\gamma')^2+4|\alpha|^2}$. These eigenstates carry z orbital angular momentum,

$$\langle\psi_1|L_z|\psi_1\rangle = -\langle\psi_2|L_z|\psi_2\rangle = \frac{2|\alpha|^2-(\gamma-\gamma')^2-(\gamma-\gamma')r}{4|\alpha|^2+(\gamma-\gamma')^2+(\gamma-\gamma')r}. \tag{3}$$

Hence, $L_z^{\rm cf}=|\langle\psi_1|L_z|\psi_1\rangle|$ depends only on the difference $(\gamma-\gamma')/|\alpha|$ and can vary from completely quenched ($L_z^{\rm cf}=0$) to unquenched ($L_z^{\rm cf}=2$). When $\gamma=\gamma'=0$, $\underline{H}^{\rm cf}$ has no diagonal matrix elements and $L_z^{\rm cf}=1/2$.

An upper orbital doublet $|\psi_{4,5}\rangle$ is obtained from $|\psi_{1,2}\rangle$ by taking $r\to -r$. It is easily shown that $\langle\psi_4|L_z|\psi_4\rangle=1-\langle\psi_1|L_z|\psi_1\rangle$ and $\langle\psi_5|L_z|\psi_5\rangle=1-\langle\psi_2|L_z|\psi_2\rangle$. We also obtain a singlet $|\psi_3\rangle=|0\rangle$ with energy $\epsilon_3=0$. The condition $\epsilon^{(0)}=0$ where the singlet $|\psi_3\rangle$ crosses the lower doublet $|\psi_{1,2}\rangle$ can be rewritten as $\gamma\gamma'=|\alpha|^2$, where γ and γ' are both positive. Since $\langle\psi_3|L_z|\psi_3\rangle=0$, the z orbital angular momentum is completely quenched with $L_z^{\rm cf}=0$ when $\epsilon^{(0)}>0$ or $\gamma\gamma'>|\alpha|^2$. With the assumption that $T\ll|\epsilon^{(0)}|$, the singlet $|\psi_3\rangle$ is unoccupied when $\gamma\gamma'<|\alpha|^2$ and the doublet $|\psi_{1,2}\rangle$ is unoccupied when $\gamma\gamma'>|\alpha|^2$.

If octahedral symmetry were preserved by the crystal field, then $\gamma=\gamma'/2$ and $\alpha=\sqrt{2}\gamma$. The singlet $|\psi_3\rangle=|0\rangle$ would then be degenerate with the $L_z^{\rm cf}=1$ doublet $|\psi_1\rangle=-\sqrt{2/3}|2\rangle+\sqrt{1/3}|-1\rangle$ and $|\psi_2\rangle=\sqrt{1/3}|1\rangle+\sqrt{2/3}|-2\rangle$.[14] Within the triplet subspace $|\psi_{1,2,3}\rangle$, the orbital angular momentum $\mathbf{L}$ can be mapped onto a Heisenberg spin-1 operator. Generally, the degeneracy of the doublet and singlet states under the condition $\gamma\gamma'=|\alpha|^2$ does not imply octahedral symmetry, so $L_z^{\rm cf}\neq 1$ unless the condition $\gamma=\gamma'/2$ is also satisfied.

Within the doublet subspace $|\psi_{1,2}\rangle$, $\mathbf{L}$ cannot be mapped onto a Heisenberg spin-1/2 operator because $\langle\psi_1|L_\pm|\psi_2\rangle=0$. Since $\langle\psi_i|L_z|\psi_i\rangle=\pm L_z^{\rm cf}$ for $i=1$ or 2, $\mathbf{L}$ can be mapped onto an Ising spin-1/2 operator within this subspace. Consequently, the spin-orbit term $\lambda\mathbf{L}\cdot\mathbf{S}$ does not contain any off-diagonal matrix elements in the $|\psi_{1,2}\rangle$ subspace.

We have performed a rough calculation of the crystal-field potential based on the oxygen positions for a Mn(II)Cr(III) system,[4] assuming that each of the oxygen positions has the same charge. Using density-functional theory to integrate over the d orbitals of a single Fe(II) atom, we find $\gamma/|\alpha|\approx 0.42$, $\gamma'/|\alpha|\approx 0.64$, and $L_z^{\rm cf}\approx 0.66$. Since $\gamma\gamma'/|\alpha|^2\approx 0.27\ll 1$, the orbital doublet is expected to lie much lower in energy than the singlet. The possible importance of this multiplet splitting for the properties of the bimetallic oxalates was first suggested by Nuttall and Day.[11]

III. TRANSITION TEMPERATURE AND MAGNETIZATION

For a magnetically anisotropic material with $\epsilon^{(0)}<0$ and $L_z^{\rm cf}>0$, the magnetic moments $M=\langle 2S_z+L_z\rangle$ and $M'=\langle 2S_z'\rangle$ on the Fe(II) and Fe(III) sites are solved within the mean-field (MF) theory. In addition to the exchange $J_c\mathbf{S}\cdot\mathbf{S}'$ and spin-orbit $\lambda\mathbf{L}\cdot\mathbf{S}$ interactions, we also include an external field $\mathbf{H}$, which contributes energies $-\mu_B\mathbf{H}\cdot(2\mathbf{S}+\mathbf{L})$ and $-2\mu_B\mathbf{H}\cdot\mathbf{S}'$. For $\mathbf{H}$ along the z axis, the effective MF Hamiltonians on the Fe(II) and Fe(III) sites are

$$H_{\rm II} = \lambda\mathbf{L}\cdot\mathbf{S} + 3J_c\langle S_z'\rangle S_z - h(S_z+L_z/2), \tag{4}$$

$$H_{\rm III} = 3J_c\langle S_z\rangle S_z' - hS_z', \tag{5}$$

where $h=2\mu_B H$ and we subtract the crystal-field energy $\epsilon^{(0)}$.

Because the exchange, spin-orbit, and external-field energies are all much smaller than $|\epsilon^{(0)}|$, the singlet state may be neglected when evaluating $H_{\rm II}$. Since the matrix elements of $L_\pm$ vanish in the subspace of the low-energy doublet, the spin-orbit interaction $\lambda\mathbf{L}\cdot\mathbf{S}$ on the Fe(II) site is diagonal. Hence, the eigenvalues of $H_{\rm II}$ in the $|\psi_{1\sigma}\rangle$, $|\psi_{2\sigma}\rangle$ subspace are

$$\epsilon_{1\sigma} = (-|\lambda|L_z^{\rm cf}+3J_cM'/2-h)\sigma - hL_z^{\rm cf}/2, \tag{6}$$

$$\epsilon_{2\sigma} = (|\lambda|L_z^{\rm cf}+3J_cM'/2-h)\sigma + hL_z^{\rm cf}/2. \tag{7}$$

Notice that $\epsilon_{1\sigma}-\epsilon_{2\sigma}=-(2|\lambda|\sigma+h)L_z^{\rm cf}$. So in zero field, $\epsilon_{1\sigma}>\epsilon_{2\sigma}$ for $\sigma<0$.

The Fe(II) magnetic moment $M(T)=\langle 2S_z+L_z\rangle$ is then obtained from

$$\langle S_z\rangle = \frac{2}{Z}\sum_\sigma \sigma e^{(-3J_cM'/2+h)\sigma/T}\cosh[(|\lambda|\sigma+h/2)L_z^{\rm cf}/T], \tag{8}$$

$$\langle L_z\rangle = \frac{2L_z^{\rm cf}}{Z}\sum_\sigma e^{(-3J_cM'/2+h)\sigma/T}\sinh[(|\lambda|\sigma+h/2)L_z^{\rm cf}/T], \tag{9}$$

$$Z = 2\sum_\sigma e^{(-3J_cM'/2+h)\sigma/T}\cosh[(|\lambda|\sigma+h/2)L_z^{\rm cf}/T], \tag{10}$$

and the Fe(III) moment is given by

$$M'(T) = 2\langle S_z'\rangle = 2S'B_{S'}[(h-3J_c\langle S_z\rangle)S'/T], \tag{11}$$

where $B_{S'}(x)$ is the spin S' Brillouin function. We adopt the convention that $M'>0$ and $M<0$ in zero field.

It is then straightforward to self-consistently evaluate the critical temperature T_c from the expression

$$\left(\frac{T_c}{J_c}\right)^2 = \frac{105}{2}\frac{\cosh(\lambda L_z^{\rm cf}/T_c)+4\cosh(2\lambda L_z^{\rm cf}/T_c)}{1+2\cosh(\lambda L_z^{\rm cf}/T_c)+2\cosh(2\lambda L_z^{\rm cf}/T_c)}. \tag{12}$$

As shown in Fig. 2, T_c/J_c is a function only of $|\lambda|L_z^{\rm cf}/J_c$ that monotonically increases from $\sqrt{S(S+1)S'(S'+1)}\approx 7.25$

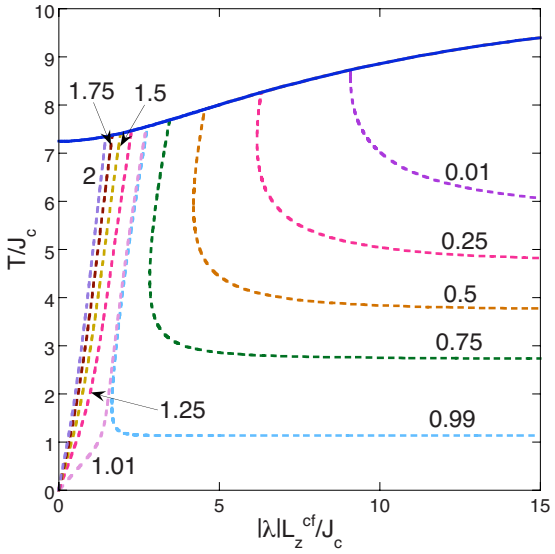

FIG. 2. (Color online) The ferrimagnetic (thick blue line) and compensation (dashed lines) temperatures versus $|\lambda|L_z^{\rm cf}/J_c$ for various values of $L_z^{\rm cf}$.

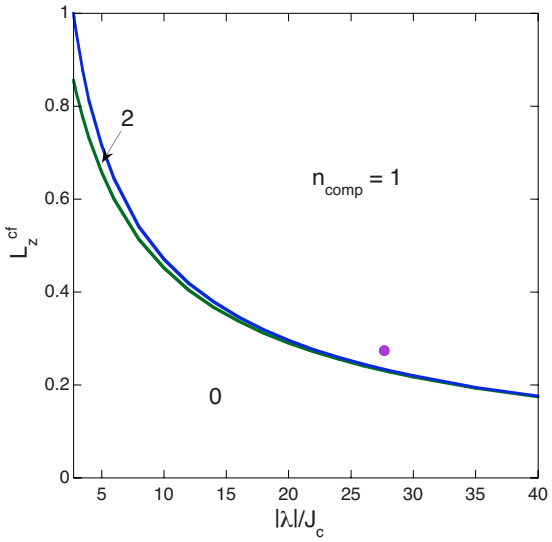

FIG. 3. (Color online) The number of compensation points $n_{\rm comp}$ in the $\{L_z^{\rm cf},|\lambda|/J_c\}$ phase space for $|\lambda|/J_c>2.75$. There is a narrow region with two compensation points between regions with $n_{\rm comp}=0$ and 1. The dotted point indicates the estimate for GNM materials.

when $|\lambda|L_z^{\rm cf}/J_c=0$ to $\sqrt{3S'(S'+1)}S\approx 10.25$ as $|\lambda|L_z^{\rm cf}/J_c\to\infty$. These results are qualitatively similar to those obtained from a MF treatment of a two-dimensional ferrimagnetic Ising model with single-ion anisotropy.[19,20] Due to two-dimensional fluctuations not considered within MF theory, the true critical temperature of a single bimetallic layer must vanish as $|\lambda|L_z^{\rm cf}\to 0$. However, the presence of a gap in the fluctuation spectrum (see Sec. V) implies that the MF theory should be fairly accurate for strong spin-orbit coupling.[16] Even for weak spin-orbit coupling, a small magnetic coupling between adjacent bimetallic planes will cut off two-dimensional fluctuations and produce a transition temperature close to the MF result.

The weak dependence of T_c/J_c on $L_z^{\rm cf}$ for large $|\lambda|L_z^{\rm cf}/J_c$ explains why all Fe(II)Fe(III) compounds that exhibit magnetic compensation have transition temperatures within a few degrees of each other, i.e., between 45 and 48 K. Due to two-dimensional fluctuations, bimetallic oxalates with smaller values of $L_z^{\rm cf}$ may have much lower critical temperatures that sensitively depend on the interlayer coupling. For example, the metallic Mn(II)Cr(III) compound with A =BEDT-TTF and very large layer separation l=16.6 Å ferromagnetically orders at a rather low 5.5 K.[7]

A similar formalism was developed some time ago by Slonczewski[21] to describe the annealing effect in Co-doped magnetite. Due to the trigonal Co(II) environment, the d levels split into two orbital doublets and a singlet. Since Co-doped magnetite is a ferromagnet, the spin-orbit coupling is not associated with magnetic compensation.

In an earlier work,[17] we demonstrated that the average magnetic moment $M^{\rm av}=(M+M')/2=(|M'|-|M|)/2$ in zero field exhibits magnetic compensation in distinct regions of $\{L_z^{\rm cf},|\lambda|/J_c\}$ phase space. If $n_{\rm comp}$ is the number of compensation points where $M^{\rm av}$ changes sign, then two regions have $n_{\rm comp}=1$: one for $|\lambda|/J_c>2.75$ and $L_z^{\rm cf(2)}<L_z^{\rm cf}<1$; the other for $|\lambda|/J_c<2.75$ and $1<L_z^{\rm cf}<L_z^{\rm cf(3)}$. In the former region, the moment is negative just below T_c where the Fe(II) moment dominates and is positive at low temperatures where the Fe(III) moment dominates; in the latter region, the moment is positive just below T_c where the Fe(III) moment dominates and is negative at low temperatures where the Fe(II) moment dominates.

These distinct regions can be seen in Fig. 2, where $T_{\rm comp}(|\lambda|L_z^{\rm cf}/J_c,L_z^{\rm cf})$ has two solutions in a narrow window of $|\lambda|L_z^{\rm cf}/J_c$ for $L_z^{\rm cf}<1$. Notice that the compensation temperature approaches a constant as $|\lambda|L_z^{\rm cf}/J_c\to\infty$ for $L_z^{\rm cf}<1$ and vanishes as $|\lambda|L_z^{\rm cf}/J_c\to 0$ for $L_z^{\rm cf}>1$. For $L_z^{\rm cf}=0.99$ and 1.01 on either side of 1, the compensation temperatures track each other down to about $2J_c$ before deviating. As shown in Fig. 3, the narrow region of phase space $L_z^{\rm cf(1)}<L_z^{\rm cf}<L_z^{\rm cf(2)}$, where $n_{\rm comp}=2$ marks a crossover between the $n_{\rm comp}=0$ region for $L_z^{\rm cf}<L_z^{\rm cf(1)}$ and the $n_{\rm comp}=1$ region for $L_z^{\rm cf(2)}<L_z^{\rm cf}<1$. This region becomes narrower as $|\lambda|/J_c$ increases, an effect which can also be seen in Fig. 2.

For large $|\lambda|/J_c>2.75$ and $L_z^{\rm cf(2)}<L_z^{\rm cf}<1$, magnetic compensation is produced by the rapid rise in the moment $|M(T)|$ on the Fe(II) sites below T_c due to the strong parallel spin-orbit coupling between $\mathbf{S}$ and $\mathbf{L}$. Just below T_c, $|M(T)|$ increases more rapidly than the spin-5/2 Brillouin function $|M'(T)|$. However, at $T=0$, the saturated moment $|M'(0)|$ =5 on the Fe(III) sites is larger than $|M(0)|=4+L_z^{\rm cf}$ on the Fe(II) sites. So the average moment must change sign at some intermediate temperature. For small $|\lambda|/J_c<2.75$ and $1<L_z^{\rm cf}<L_z^{\rm cf(3)}$, magnetic compensation occurs because the spin-5/2 Brillouin function increases more rapidly than the spin-2 Brillouin function just below T_c but $|M(0)|>|M'(0)|$ due to the orbital contribution on the Fe(II) sites.

The dominant role played by the organic cations in Fe(II)Fe(III) bimetallic oxalates is to alter the crystal-field potential by shifting the Fe(II) ions with respect to the oxalate molecules. By contrast, the sign of the exchange coupling through the oxalate bridge is determined by the d-level

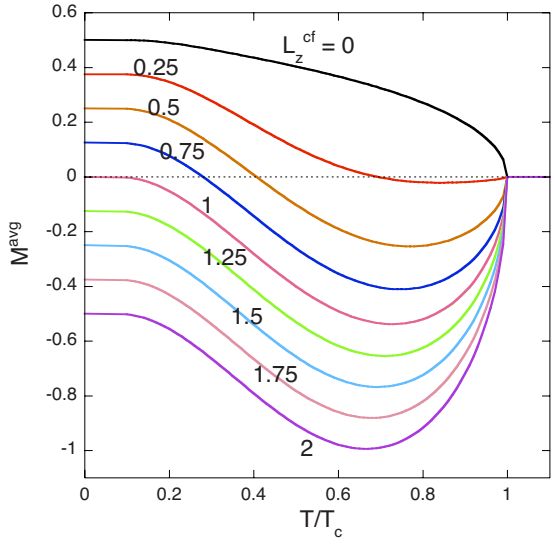

FIG. 4. (Color online) The average magnetic moment on the Fe(II) and Fe(III) sites versus T/T_c for various L_z^{cf} and $\lambda/J_c=-27.5$. The Fe(III) moment is defined to be positive.

occupation of the transition metals and the spin-orbit coupling is an atomistic effect. Thus, both are unaffected by the choice of cation A.

Normal Fe(II)Fe(III) bimetallic oxalates without magnetic compensation can fall into two classes. The organic cations may reverse the distortion of the C_3-symmetric crystal field so that $\epsilon^{(0)}>0$ with the $L_z^{\mathrm{cf}}=0$ singlet lying lower in energy than the orbital doublet. Because there is no magnetic anisotropy when $L_z^{\mathrm{cf}}=0$, GNM would be absent as well. Alternatively, the orbital doublet may remain lower in energy but with a small $L_z^{\mathrm{cf}}>0$ falling into the first $n_{\mathrm{comp}}=0$ region.

Our results for T_{comp} and T_c can be used to estimate the experimental parameters for bimetallic oxalates that exhibit GNM. Taking the value of $\lambda\approx-102$ cm^{-1} or -12.65 meV from paramagnetic resonance measurements of Fe(II)[22,23] and the estimate $T_{\mathrm{comp}}/T_c=0.62$ from experiments on GNM materials,[10] we obtain $J_c\approx0.46$ meV and $L_z^{\mathrm{cf}}\approx0.274$. This point is indicated by a dot in Fig. 3. For $\lambda/J_c=-27.5$, $L_z^{\mathrm{cf}(1)}=0.228$ and $L_z^{\mathrm{cf}(2)}=0.232$. Hence, GNM materials lie just inside the first $n_{\mathrm{comp}}=1$ region for $L_z^{\mathrm{cf}(2)}<L_z^{\mathrm{cf}}<1$. Mössbauer spectroscopy[10,12] confirms that the Fe(II) moment in GNM compounds dominates just below T_c, as anticipated for this region of phase space.

Using $\lambda=-27.5J_c$, M^{av} is plotted versus T/T_c for various values of L_z^{cf} in Fig. 4, where the magnetic moment of Fe(III) is chosen to be positive. When $0\le L_z^{\mathrm{cf}}<L_z^{\mathrm{cf}(1)}=0.228$, there are no compensation points and the average moment is always positive [the Fe(III) moment is always larger in magnitude than the Fe(II) moment]. In the narrow region between $L_z^{\mathrm{cf}(1)}=0.228$ and $L_z^{\mathrm{cf}(2)}=0.232$, there are two compensation temperatures. For $L_z^{\mathrm{cf}(2)}<L_z^{\mathrm{cf}}<1$, there is a single compensation temperature above which the average moment is negative [Fe(II) has the larger absolute moment]. For $1<L_z^{\mathrm{cf}}\le2$, the average moment is always negative [Fe(II) always has a larger absolute moment due to its orbital contribution]. Whereas the values of L_z^{cf} for all other GNM compounds are believed to fall between $L_z^{\mathrm{cf}(2)}$ and 1, it is possible that L_z^{cf} for the bimetallic oxalate studied in Ref. 13 falls within the narrow window between $L_z^{\mathrm{cf}(1)}$ and $L_z^{\mathrm{cf}(2)}$ with $n_{\mathrm{comp}}=2$.

In the absence of spin-orbit coupling, a Jahn–Teller (JT) distortion of the oxygen atoms around each Fe(II) would gain electronic energy by splitting the low-energy doublet. In the presence of spin-orbit coupling, a JT distortion would mix the eigenstates $|\psi_{1\sigma}\rangle$ and $|\psi_{2\sigma}\rangle$, thereby lowering the orbital angular momentum of the doublet. Due to the competition between the spin-orbit and electronic energies,[14] the JT distortion will be quenched unless the spring constant of the oxygen atoms is sufficiently weak. Consequently, JT distortions are commonly neglected in systems with nonquenched orbital angular momentum. However, even in the absence of a JT distortion, the organic cations may themselves induce a non-C_3-symmetric distortion of the crystal field about each Fe(II) ion. We recently proposed that one of the two compensation temperatures observed by Tang *et al.*[13] is actually caused by an inverse JT distortion[24] from a nondistorted phase at low temperatures to a distorted phase at intermediate temperatures. The general effects of a crystal-field distortion that violates C_3 symmetry are discussed in Sec. VI.

The persistence of negative magnetization in small positive fields is associated both with the finite energy barrier $2|\lambda|L_z^{\mathrm{cf}}S$ for flipping $\langle L_z\rangle$ once it is aligned parallel to the magnetic field and with the small matrix element for this dipole-allowed transition [due to the hybridization of the $L=2$ and $L=1$ wave functions by the nonspherical crystal-field potential $V(\rho,\theta,\phi)$]. By optically exciting the higher-energy state of the orbital doublet with near-infrared light of frequency $2|\lambda|L_z^{\mathrm{cf}}S\approx14$ meV or wavelength of 88.5 μm, it should be possible to flip the magnetic moment in a negative-magnetization state below T_{comp}. This optical effect would be maximized if the magnetic field lies just below the critical field required to flip the magnetization. Optical control of the magnetization has been previously demonstrated in a Mn(II)Cr(III) bimetallic oxalate[5] and other organic magnets.[25]

It seems likely that the difference between the zero-field-cooled and field-cooled susceptibilities of GNM materials[26] is produced by the flipping of clusters of Fe moments in an applied field. The anomalous decrease in the susceptibility with applied field[26] can be explained by the reduction in the net magnetic moment associated with the flipping of some clusters.

An alternative explanation for magnetic compensation in the bimetallic oxalates is provided, as in the rare-earth/transition-metal intermetallics,[27] by next-nearest-neighbor interactions between moments on the same sublattice. While Carling and Day[28] obtain a very good fit to the experimental data using just nearest-neighbor and next-neighbor interactions [coupling the Fe(II) moments only] between Ising spins on an open honeycomb lattice, their model cannot explain either the increase in T_c with layer separation l in the $A=\mathrm{N}(n\text{-}\mathrm{C}_n\mathrm{H}_{2n+1})_4$ family or the negative magnetization below T_{comp}. They also require a rather larger ferromagnetic coupling (roughly half the antiferromagnetic nearest-neighbor coupling) between the Fe(II) moments to explain the experimental measurements.

The two compensation points in Prussian Blue analogs can be explained[29] within the MF theory by the presence of four species of spins, coupled by one antiferromagnetic and two different ferromagnetic interactions. Multiple compensation points also arise in an effective-field theory of a "decorated" ferrimagnetic Ising model with next-neighbor interactions and single-ion anisotropy.[30]

Recent Monte Carlo simulations[31] imply that the magnetic compensation predicted by the ferrimagnetic Ising model on an open honeycomb lattice is an artifact of using MF theory[19,20] to treat both the exchange interaction between the neighboring spins and the single-ion anisotropy at the Fe(II) sites. Magnetic compensation then requires either an interlayer coupling or a longer-ranged interaction within the plane. Within our model, the negative magnetization of a single bimetallic plane has three origins: the effective anisotropic field at the Fe(II) sites produced by the spin-orbit coupling and crystalline field, the orbital contribution to the total magnetic moment at the Fe(II) sites, and the energy barrier for flipping the Fe(II) orbital angular momentum. The latter two effects are absent in an Ising ferrimagnet. We have used the MF theory to approximate the exchange coupling $J_c\mathbf{S}\cdot\mathbf{S}'$ between neighboring Fe(II) and Fe(III) moments but not the spin-orbit coupling $\lambda\mathbf{L}\cdot\mathbf{S}$ at the Fe(II) sites, which is evaluated exactly within the orbital doublet.

IV. MAGNETIC PHASE DIAGRAM AND MAGNETIC SUSCEPTIBILITY

We now evaluate the $T=0$ magnetic phase diagram of the Fe(II)Fe(III) bimetallic oxalates with a magnetic field $\mathbf{H}$ applied along the z axis perpendicular to the layers. The spins $\mathbf{S}$ and $\mathbf{S}'$ are treated classically. Writing the expectation values of the spins as $\langle\mathbf{S}\rangle = S(-\cos\theta, 0, \sin\theta)$ and $\langle\mathbf{S}'\rangle = S'(\cos\psi, 0, \sin\psi)$, we obtain effective MF Hamiltonians on the Fe(III) and Fe(III) sites, as follows:

$$H_{\mathrm{II}} = (\lambda\langle L_z\rangle - h + 3J_cS'\sin\psi)S_z + 3J_cS'\cos\psi\, S_x \equiv -\mathbf{h}_{\mathrm{eff}}\cdot\mathbf{S}, \tag{13}$$

$$H_{\mathrm{III}} = (3J_cS\sin\theta - h)S'_z - 3J_cS\cos\theta\, S'_x \equiv -\mathbf{h}'_{\mathrm{eff}}\cdot\mathbf{S}'. \tag{14}$$

With a correction to avoid double counting, the energy can be written

$$\frac{1}{N}E(\theta,\psi,\langle L_z\rangle) = -\langle L_z\rangle(|\lambda|S\sin\theta + h/2) - h(S\sin\theta + S'\sin\psi) - 3J_cSS'\cos(\theta+\psi), \tag{15}$$

where N is the number of Fe(II) or Fe(III) sites.

Minimizing E with respect to $\langle L_z\rangle$, we find that $\langle L_z\rangle = \pm L_z^{\mathrm{cf}}$, where the + sign is for $h > -2|\lambda|S\sin\theta$ and the − sign is for $h < -2|\lambda|S\sin\theta$. Thus, for $\langle\mathbf{S}\rangle$ pointing down ($\sin\theta < 0$), a positive field is required to flip the orbital angular momentum from down to up.

The equilibrium values of θ and ψ are obtained either by minimizing $E(\theta,\psi)$ or from the conditions that $\langle\mathbf{S}\rangle$ and $\langle\mathbf{S}'\rangle$ are parallel to the effective fields $\mathbf{h}_{\mathrm{eff}}$ and $\mathbf{h}'_{\mathrm{eff}}$, respectively, as in

$$-\cot\theta = \frac{3J_cS'\cos\psi}{\lambda\langle L_z\rangle + 3J_cS'\sin\psi - h}, \tag{16}$$

$$\cot\psi = \frac{-3J_cS\cos\theta}{3J_cS\sin\theta - h}. \tag{17}$$

There are two critical fields: $H_{c1} = h_{c1}/(2\mu_B)$ and $H_{c2} = h_{c2}/(2\mu_B)$. For $0 < h < h_{c1}$, the Fe(II) and Fe(III) spins are antiparallel along the $\pm z$ directions. For $h_{c1} < h < h_{c2}$, the spins are canted with $-\pi < \theta < \pi$ and $-\pi < \psi < \pi$. Above h_{c2}, the spins are aligned along the z axis with $\theta = \psi = \pi/2$.

The magnetic phase diagrams are slightly different for $L_z^{\mathrm{cf}} < 1$ and $L_z^{\mathrm{cf}} > 1$. When $L_z^{\mathrm{cf}} > 1$, $\langle L_z\rangle$ always points along the field direction. As shown in Fig. 5(a) for $L_z^{\mathrm{cf}} = 1.5$, the transition at h_{c1} involves only the canting of the spins and not the reversal of $\langle L_z\rangle$. On the other hand, for $L_z^{\mathrm{cf}} < 1$, the orbital angular momentum points opposite the field direction in small fields. For large enough $|\lambda|/J_c$, $\langle L_z\rangle$ reverses direction at the same field as the spin-flop transition. However, for very small $|\lambda|/J_c$, the orbital angular momentum can reverse direction independent of the spins, as shown in the inset of Fig. 5(b) for $L_z^{\mathrm{cf}} = 0.5$. For $|\lambda|/J_c > 0.16$ and $L_z^{\mathrm{cf}} = 0.5$, the transition at h_{c1} is a cooperative transition involving both the

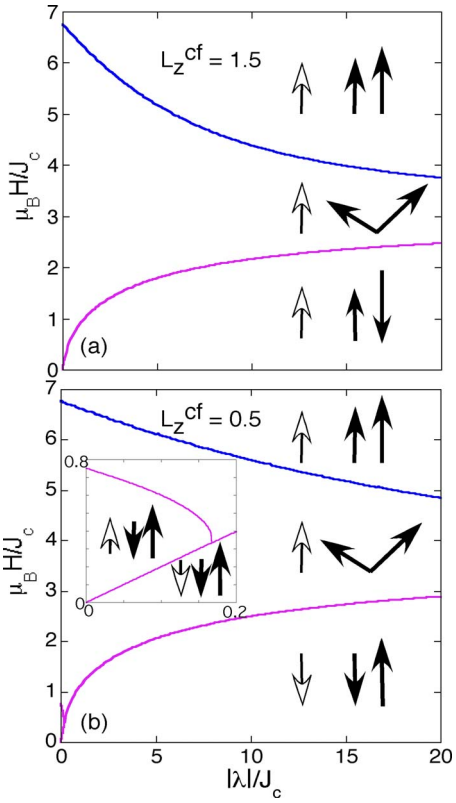

FIG. 5. (Color online) The magnetic phase diagram for (a) $L_z^{\mathrm{cf}} = 1.5$ and (b) 0.5, where the hollow arrows denote $\langle\mathbf{L}\rangle$ and the adjacent solid arrows denote $\langle\mathbf{S}\rangle$ and $\langle\mathbf{S}'\rangle$. For small $|\lambda|/J_c$ and $L_z^{\mathrm{cf}} < 1$, the orbital angular momentum can flip independent of the spins, as shown in the inset of (b).

reversal of $\langle L_z \rangle$ and the canting of the spins. As discussed in the next section, the cooperative nature of this spin-flop transition has important consequences for the SW spectrum. Using the estimates $L_z^{\rm cf} \approx 0.27$ and $|\lambda|/J_c \approx 27.5$, we find that $\mu_B H_{c1} \approx 3J_c$, which corresponds to a critical field of about 24 T.

Returning to a quantum description of the spins $\mathbf{S}$ and $\mathbf{S}'$, the magnetic susceptibility $\chi = 2\mu_B M^{\rm av}/H$ approaches the form $C/(T-\Theta)$ in the high-temperature limit $T \gg |\lambda| L_z^{\rm cf} S$, with the Curie constant

$$C = \frac{4}{3}\mu_B^2 \{S(S+1) + S'(S'+1)\} + (L_z^{\rm cf}\mu_B)^2. \tag{18}$$

Both $\mathbf{S}$ and $\mathbf{S}'$ contribute factors of 4/3 because they are three-dimensional Heisenberg spins that couple to the magnetic field with a coefficient of $2\mu_B$. By contrast, the orbital angular momentum $\mathbf{L}$ of the orbital doublet is an Ising variable that couples to the magnetic field with a factor of μ_B. Our result for C implies that GNM materials with $L_z^{\rm cf} > L_z^{\rm cf(2)}$ will have higher Curie constants than normal materials with $L_z^{\rm cf} < L_z^{\rm cf(1)}$. However, the difference is rather small due to the much larger contributions of the spins $S=2$ and $S'=5/2$. Using the values estimated above for a GNM compound, we would find $C \approx 19.74\mu_B^2$, just slightly larger than the $L_z^{\rm cf}=0$ value of $(59/3)\mu_B^2 \approx 19.67\mu_B^2$.

Also in the high-temperature limit, the Curie temperature Θ is given by

$$\Theta C = -\frac{8}{3}\mu_B^2 S(S+1)S'(S'+1)J_c + \frac{4}{3}|\lambda|(L_z^{\rm cf}\mu_B)^2 S(S+1), \tag{19}$$

which is negative because the antiferromagnetic contribution of the first term dominates. By enhancing the magnetic susceptibility, the spin-orbit coupling lowers the absolute value $|\Theta|$. Within the MF theory, $|\Theta|$ must be less than or equal to the critical temperature T_c and the two are equal only for an antiferromagnet without spin-orbit coupling: $S=S'$ and $|\lambda|=0$. Using the parameters estimated above for a GNM material, $\Theta C/\mu_B^2 \approx -57$ meV and $\Theta \approx -33.5$ K. Equation (19) also implies that $|\Theta|$ is smaller in GNM compounds with larger values of $|\lambda|(L_z^{\rm cf})^2$.

However, $|\Theta|$ exceeds 85 K in most normal Fe(II)Fe(III) compounds and $|\Theta|$ can be as large as 145 K in some GNM compounds.[10,12] This suggests that fluctuations may substantially suppress the critical temperature from its MF value and that J_c is significantly larger than the value of 0.46 meV estimated above.[11] It is much more difficult to understand the enhanced value of the Curie constant in GNM materials, which is typically about 20% larger than in normal compounds.[10]

The authors of Ref. 10 have noted the presence of Fe oxide impurities in the GNM samples. If GNM samples are contaminated with Fe oxides, then the total susceptibility would be the sum of the pure material plus that of the contaminant. This would increase the effective Curie constant while lowering the apparent compensation temperature. Hence, it is possible that GNM materials lie even closer to the $n_{\rm comp}=0$ phase boundary $L_z^{\rm cf(1)}=0.23$ than estimated in Sec. III using $T_{\rm comp}/T_c \approx 0.62$.

V. SPIN-WAVE SPECTRUM

To evaluate the SW spectrum, we start with the spin Hamiltonian for a bimetallic layer in the presence of a magnetic field $h=2\mu_B H$, which is perpendicular to the bimetallic layers. Assuming that either $\langle L_z \rangle = -L_z^{\rm cf}$ $(0 \le L_z^{\rm cf} < 1)$ or $\langle L_z \rangle = L_z^{\rm cf}$ $(1 < L_z^{\rm cf} \le 2)$,

$$H^{\rm spin} = \lambda \langle L_z \rangle \sum_i S_{iz} + J_c \sum_{\langle i,j \rangle} \mathbf{S}_i \cdot \mathbf{S}'_j - h\{\sum_i S_{iz} + \sum_j S'_{iz}\}, \tag{20}$$

where sites i or j are on the Fe(II) or Fe(III) sublattice, respectively. If $\langle L_z \rangle = +$ (or $-$) $L_z^{\rm cf}$, then the Fe(II) spins point up (or down) for fields $h < h_{c1}$.

Only fluctuations of the spin are considered. Unlike the spin, $L_z = \pm L_z^{\rm cf}$ is an Ising degree of freedom within the orbital doublet. Thus, fluctuations of the orbital degrees of freedom require energy $2|\lambda|L_z^{\rm cf} S \approx 14$ meV, which is much higher than the minimum energy for spin fluctuations. Because orbital fluctuations are much slower than spin fluctuations, the latter may be evaluated for an average orbital occupation $\langle L_z \rangle$. The orbital term in $H^{\rm spin}$ acts to shift the effective field on the Fe(II) site from h to $h - \lambda\langle L_z \rangle$.

We perform a Holstein–Primakoff expansion about the classical-spin limit to evaluate the SW frequencies of a Fe(II)Fe(III) bimetallic oxalate. Since the spins S and S' are fairly large, this expansion will incur relatively small errors of order $1/(2S+1)=1/5$ and $1/(2S'+1)=1/6$. For $L_z^{\rm cf} < 1$, the Fe(II) spins and orbital angular momentum point down for small fields while the Fe(III) spins point up. Thus, we transform to the boson operators a_i and b_i using $S_{iz} = -S + a_i^\dagger a_i$, $S_{i+} = \sqrt{2S}a_i^\dagger$, $S_{i-} = \sqrt{2S}a_i$, $S'_{jz} = S' - b_j^\dagger b_j$, $S'_{j+} = \sqrt{2S'}b_j$, and $S'_{j-} = \sqrt{2S'}b_j^\dagger$. For $L_z^{\rm cf} > 1$, $\mathbf{S}_i$ and $\mathbf{S}'_j$ would be switched. To first order in $1/S$ and $1/S'$, $H^{\rm spin}$ is then diagonalized in momentum space using standard techniques.

Acoustic and optical branches of SWs are found with frequencies

$$\begin{aligned}\omega_{\mathbf{k}}^{(\pm)}(h) = & \pm\{-\lambda L_z^{\rm cf}/2 + 3J_c(S'-S)/2 + {\rm sgn}(L_z^{\rm cf}-1)h\} \\ & + \{9J_c^2(S'+S)^2/4 + (\lambda L_z^{\rm cf})^2/4 \\ & - 3\lambda L_z^{\rm cf} J_c(S'+S)/2 - 9J_c^2 SS'|\gamma_{\mathbf{k}}|^2\}^{1/2},\end{aligned} \tag{21}$$

where

$$\gamma_{\mathbf{k}} = \frac{1}{3}\{e^{ik_x a} + 2e^{-ik_x a/2}\cos(\sqrt{3}k_y a/2)\} \tag{22}$$

and a is the separation between neighboring Fe(II) and Fe(III) ions. Notice that $\gamma_{\mathbf{k}=0}=1$. Due to the change in spin orientation, the sign multiplying the magnetic field depends on whether $L_z^{\rm cf}$ is greater or less than 1.

For the parameters estimated above, the zero-field SW frequencies are plotted versus $k_x a$ in Fig. 6. The Brillouin zone for the open honeycomb structure has width $4\pi/3a$

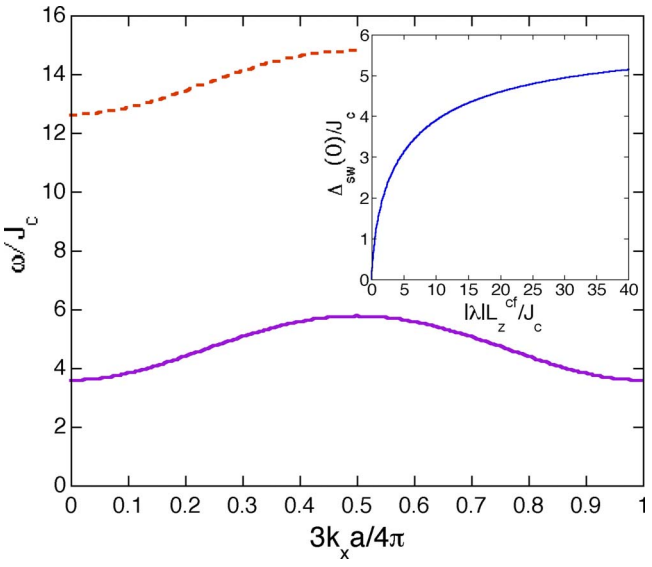

FIG. 6. (Color online) The SW frequencies ω/J_c versus $k_x a$ for $L_z^{\mathrm{cf}}=0.27$ and $|\lambda|/J_c=27.5$. The inset is the zero-field SW gap $\Delta_{\mathrm{sw}}(0)/J_c$ versus $|\lambda|L_z^{\mathrm{cf}}/J_c$.

along the k_x axis. The dispersion along k_x is rather modest with a change of about $1.5J_c \approx 0.7$ meV across the Brillouin zone.

The lower of the two SW frequencies at $\mathbf{k}=0$ gives the SW gap $\Delta_{\mathrm{sw}}(h)$. As shown in the inset of Fig. 6, the zero-field SW gap $\Delta_{\mathrm{sw}}(h=0)=\omega_{\mathbf{k}=0}^{(-)}(h=0)$ vanishes like $|\lambda|L_z^{\mathrm{cf}}S/(S'-S)$ as $|\lambda|L_z^{\mathrm{cf}}\to 0$ and approaches $3J_cS$ as $|\lambda|L_z^{\mathrm{cf}}/J_c\to\infty$. Using the parameters estimated above, we obtain $\Delta_{\mathrm{sw}}(0)\approx 1.65$ meV. This should be relatively simple to observe with inelastic neutron-scattering techniques. The SW gap explains the high transition temperatures of well-separated two-dimensional layers, where gapless spin excitations would suppress the critical temperature.[16] Our results imply that GNM materials will have larger SW gaps than normal materials.

According to Eq. (20), the spin-orbit coupling within each layer stabilizes the ferrimagnetic order of Fe(II)Fe(III) bimetallic oxalates. Since the coupling between layers is assumed to be negligible, the SWs do not disperse along the k_z direction. This conclusion can be tested by performing inelastic neutron-scattering measurements on a single crystal.

As emphasized in the previous section, the spin-flop for $L_z^{\mathrm{cf}}<1$ is a cooperative transition involving both the reversal of the orbital angular momentum as well as the canting of the spins. Thus, the SW gap evaluated with $\langle L_z\rangle=-L_z^{\mathrm{cf}}$ does not vanish at H_{c1} when $L_z^{\mathrm{cf}}<1$. By contrast, the SW gap does vanish at the spin-flop transition when $L_z^{\mathrm{cf}}>1$ since $\langle L_z\rangle=L_z^{\mathrm{cf}}$ is always aligned with the magnetic field. In this case, the spin-flop transition only involves the canting of the spins and not the reversal of the orbital angular momentum. Hence, the critical field H_{c1} in Fig. 5(a) satisfies the condition $\Delta_{\mathrm{sw}}(h)=\omega_{\mathbf{k}=0}^{(-)}(h)=0$ so that $h_{c1}\to 6J_c$ or $\mu_B H_{c1}\to 3J_c$ as $|\lambda|L_z^{\mathrm{cf}}/J_c\to\infty$.

VI. CRYSTAL-FIELD DISTORTIONS

In the absence of the spin-orbit energy, a distortion of the oxygen triangles that violates C_3 symmetry would split the low-energy orbital doublet into the nondegenerate levels $|\psi_\sigma^{\pm}\rangle=(1/\sqrt{2})(|\psi_{1\sigma}\rangle\pm|\psi_{2\sigma}\rangle)$ with $\langle L_z\rangle=0$.[14] Since the spin-orbit coupling favors a nonquenched orbital ground state, it maintains a ground-state doublet with nonzero orbital angular momenta. Distortions of the oxygen triangles can occur spontaneously due to the JT effect.[24] However, if the elastic-energy cost for the displacement of the oxygen atoms is sufficiently large, then the JT distortion would be quenched by the spin-orbit coupling and the local C_3 symmetry would be preserved. It is also possible that the local crystal field violates C_3 symmetry due to the shape of the cations themselves. This is the case for at least one bimetallic oxalate,[12] where the $Mn(II)_3Fe(III)_3$ hexagons are distorted because the $FeCp_2^*$ organic cations violate C_3 symmetry. Another possibility, discussed further below, is that uniaxial strain distorts the crystal field.

Generally, the mixing of the $|\psi_{1\sigma}\rangle$ and $|\psi_{2\sigma}\rangle$ states can be described by the Hamiltonian

$$H^{\mathrm{mixing}}=\begin{pmatrix}\epsilon_{1\sigma} & \xi\\ \xi & \epsilon_{2\sigma}\end{pmatrix}, \tag{23}$$

where the mixing energy ξ does not depend on σ and $\epsilon_{i\sigma}$ are given by Eqs. (6) and (7). In zero field, the eigenvalues of H^{mixing} are $\epsilon_{a\sigma}=3J_cM'\sigma/2+t_\sigma$ and $\epsilon_{b\sigma}=3J_cM'\sigma/2-t_\sigma$ with $t_\sigma=-\mathrm{sgn}(\sigma)\sqrt{(\lambda L_z^{\mathrm{cf}}\sigma)^2+\xi^2}$.

Since the eigenstates $|\psi_{a\sigma}\rangle$ and $|\psi_{b\sigma}\rangle$ are affected by the competition between the crystal-field distortion and the spin-orbit coupling, the orbital angular momenta now depend on the spin σ,

$$L_{a\sigma}\equiv\langle\psi_{a\sigma}|L_z|\psi_{a\sigma}\rangle=(L_z^{\mathrm{cf}})^2\lambda\sigma\frac{\lambda L_z^{\mathrm{cf}}\sigma+t_\sigma}{(\lambda L_z^{\mathrm{cf}}\sigma)^2+\lambda L_z^{\mathrm{cf}}\sigma t_\sigma+\xi^2}, \tag{24}$$

and $L_{b\sigma}\equiv\langle\psi_{b\sigma}|L_z|\psi_{b\sigma}\rangle=-L_{a\sigma}$. In the absence of magnetic order, the spin $\mathbf{S}$ and orbital angular momentum $\mathbf{L}$ are parallel for the degenerate, low-energy doublets $|\psi_{a\sigma}\rangle$ and $|\psi_{b,-\sigma}\rangle$ and antiparallel for the degenerate, high-energy doublets $|\psi_{a,-\sigma}\rangle$ and $|\psi_{b\sigma}\rangle$ with $\sigma=1$ and 2. In the presence of magnetic order, the degeneracy of each Kramer's doublet is lifted. Notice that $L_{a,\sigma=0}=L_{b,\sigma=0}=0$ due to the absence of spin-orbit coupling when $\sigma=0$. In terms of t_σ, the transition temperature is given by the self-consistent relation

$$\left(\frac{T_c}{J_c}\right)^2=\frac{105}{2}\frac{\cosh(t_1/T_c)+4\cosh(t_2/T_c)}{\cosh(t_0/T_c)+2\cosh(t_1/T_c)+2\cosh(t_2/T_c)}, \tag{25}$$

which generalizes Eq. (12).

For the estimated parameters of a GNM material, the absolute values $L_z^{\mathrm{cf}}(\sigma,\xi)=|L_{a\sigma}|=|L_{b\sigma}|$ and T_c/J_c are plotted versus ξ/J_c in Figs. 7(a) and 7(c). As expected, the mixing energy suppresses the orbital angular momentum of the Kramer doublets with $\sigma=\pm 1$ and ± 2. By suppressing the effects of the spin-orbit coupling, the mixing also lowers T_c. Correspondingly, the crystal-field distortion increases the compensation temperature, as shown in Fig. 7(b). Magnetic compensation disappears when ξ exceeds about $10.6J_c\approx 4.8$ meV. At this value, T_c is reduced by almost 2.5%.

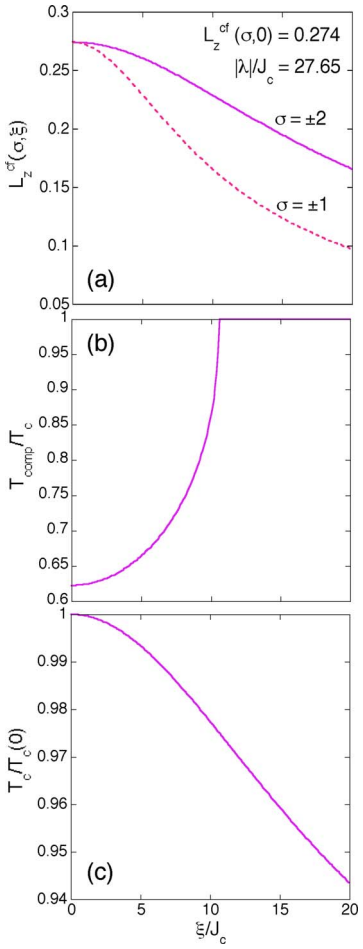

FIG. 7. (Color online) The effect of the mixing energy ξ on (a) the orbital angular momentum of the Kramer doublets with $\sigma = \pm 1$ and ± 2, (b) the compensation temperature normalized by T_c, and (c) the transition temperature T_c.

A uniaxial lattice distortion along the x or y axis plays the same role as the crystal-field distortion discussed above. If $V^{\text{strain}} = \eta(x^2 - y^2) \propto \eta \cos 2\phi \sin^2 \theta$, then $|\psi_{1\sigma}\rangle$ and $|\psi_{2\sigma}\rangle$ are coupled by a mixing energy ξ proportional to η. Therefore, uniaxial strain will increase the compensation temperature of a GNM compound. With the temperature fixed at T_{comp}, uniaxial strain will cause the magnetization to become negative.

VII. CONCLUSION

This work has provided a pathway whereby structural information can be used to design the magnetic properties of an important class of layered, molecule-based magnets. Fe(II)Fe(III) bimetallic oxalates with compensation temperatures in specified ranges are associated with corresponding ranges of L_z^{cf}, which are produced by cations with the appropriate crystal-field parameters $\gamma/|\alpha|$ and $\gamma'/|\alpha|$. With the help of first-principles calculations, it may one day be possible to choose intercalated cations that generate the desired crystal-field splittings and magnetic behavior.

Our study of the Fe(II)Fe(III) bimetallic oxalates has led to several new predictions. The SW gap is expected to be larger in GNM compounds than in normal materials. If the orbital doublet for a normal material lies below the singlet (but with $L_z^{\text{cf}} < L_z^{\text{cf}(1)}$ in the $n_{\text{comp}} = 0$ region of Fig. 3), then the spin-orbit coupling would still provide the dominant contribution to the magnetic anisotropy but the SW gap would be reduced. If the singlet lies below the orbital doublet, then the single-ion anisotropy rather than the spin-orbit coupling would produce the magnetic anisotropy and the SW gap would be even smaller. It may be possible to reverse the negative-magnetization state of a GNM material by using near-infrared light to flip the orbital angular momentum. The mixing of the two states in the orbital doublet by a cation-induced distortion or uniaxial strain will increase the magnetic compensation temperature. If the C_3-breaking potential is sufficiently strong, then a GNM material will become normal.

However, several questions remain unanswered by the present work. Two-dimensional fluctuations not included within the MF theory may have a large effect on the compensation and transition temperatures. How these fluctuations alter the phase diagram of Fig. 3 remains an open question. In addition, the present model cannot satisfactorily explain the enhancement of the Curie constant C in GNM materials. We hope that the present work will inspire further experimental study of the bimetallic oxalates as well as theoretical studies of other layered molecule-based magnets.

ACKNOWLEDGMENTS

We gratefully acknowledge useful conversations with Sasha Chernyshev, Eugenio Coronado, Patrik Henelius, Mark Meisel, and Juana Moreno. Our research is sponsored by the Laboratory Directed Research and Development Program of Oak Ridge National Laboratory (ORNL), which is managed by UT-Battelle, LLC for the U.S. Department of Energy under Contract No. DE-AC05-00OR22725.

[1] J. S. Miller and A. J. Epstein, MRS Bull. **25**, 21 (2000); J. S. Miller, Adv. Math. **14**, 1105 (2002).
[2] S. J. Blundell and F. L. Pratt, J. Phys.: Condens. Matter **16**, R771 (2004).
[3] H. Tamaki, Z. J. Zhong, N. Matsumoto, S. Kida, M. Koikawa, N. Achiwa, Y. Hashimoto, and H. Õkawa, J. Am. Chem. Soc. **114**, 6974 (1992).
[4] R. Pellaux, H. Schmalle, R. Huber, P. Fischer, T. Hauss, B. Ouladdiaf, and S. Decurtins, Inorg. Chem. **36**, 2301 (1997).
[5] S. Bénard, P. Yu, J. P. Audière, E. Rivière, R. Clément, J. Guilhem, L. Tchertanov, and K. Nakatani, J. Am. Chem. Soc. **122**, 9444 (2000); S. Bénard, E. Rivière, P. Yu, K. Nakatani, and J. F.

Delouis, Chem. Mater. **13**, 159 (2001).
[6] I. D. Watts, S. G. Carling, P. Day, and D. Visser, J. Phys. Chem. Solids **66**, 932 (2005).
[7] E. Coronado and J. R. Galán-Mascarós, C. J. Gómez-García, and V. Laukhin, Nature (London) **408**, 447 (2000).
[8] A. Alberola, E. Coronado, J. R. Galán-Mascarós, C. Giménez-Saiz, and C. J. Gómez-García, J. Am. Chem. Soc. **125**, 10774 (2003).
[9] C. Mathonière, S. G. Carling, D. Yusheng, and P. Day, J. Chem. Soc., Chem. Commun. **1994**, 1551.
[10] C. Mathonière, C. J. Nuttall, S. G. Carling, and P. Day, Inorg. Chem. **35**, 1201 (1996).
[11] C. J. Nuttall and P. Day, Chem. Mater. **10**, 3050 (1998).
[12] E. Coronado, J. R. Galán-Mascarós, C. J. Gómez-García, and J. M. Martinez-Agudo, Adv. Math. **11**, 558 (1999); E. Coronado, J. R. Galán-Mascarós, C. J. Gómez-García, J. Ensling, and P. Gütlich, Chem.-Eur. J. **6**, 552 (2000).
[13] G. Tang, Y. He, F. Liang, S. Li, and Y. Huang, Physica B **392**, 337 (2007).
[14] J. B. Goodenough, *Magnetism and the Chemical Bond* (Interscience, New York, 1963).
[15] M. Clemente-León, E. Coronado, J. R. Galán-Mascarós, and C. J. Gómez-García, Chem. Commun. (Cambridge) **1997**, 1727.
[16] R. P. Erickson and D. L. Mills, Phys. Rev. B **43**, 11527 (1991).
[17] R. S. Fishman and F. A. Reboredo, Phys. Rev. Lett. **99**, 217203 (2007).
[18] O. Kahn, *Molecular Magnetism* (VCH, New York, 1994).
[19] T. Kaneyoshi, Y. Nakamura, and S. Shin, J. Phys.: Condens. Matter **10**, 7025 (1998).
[20] Q. Zhang and G.-Z. Wei, J. Magn. Magn. Mater. **253**, 96 (2002).
[21] J. C. Slonczewski, Phys. Rev. **110**, 1341 (1958).
[22] B. Bleaney and K. W. H. Stevens, Rep. Prog. Phys. **16**, 108 (1953).
[23] The *p-d* hybridization with the ligands may reduce the magnitude of the spin-orbit coupling parameter λ by about 20%–30%. See J. Owen and J. H. M. Thornley, Rep. Prog. Phys. **29**, 675 (1966).
[24] R. S. Fishman, S. Okamoto, and F. A. Fernando, arXiv:0802.2678 (unpublished).
[25] See D. A. Pejaković, C. Kitamura, J. S. Miller, and A. J. Epstein, Phys. Rev. Lett. **88**, 057202 (2002), and references cited therein.
[26] A. Bhattacharjee, S. Iijima, F. Mizutani, T. Katsura, N. Matsumoto, and H. Õkawa, Jpn. J. Appl. Phys., Part 1 **34**, 1521 (1995).
[27] J. Ostoréro and M. Guillot, J. Appl. Phys. **99**, 08M305 (2006).
[28] S. G. Carling and P. Day, Polyhedron **20**, 1525 (2001).
[29] S. I. Ohkoshi, Y. Abe, A. Fujishima, and K. Hashimoto, Phys. Rev. Lett. **82**, 1285 (1999).
[30] T. Kaneyoshi, Physica A **229**, 166 (1996).
[31] Y. Nakamura, Phys. Rev. B **62**, 11742 (2000).